

Dissipation and noise in strongly driven Josephson junctions

Vasilii Vadimov¹*, Yoshiki Sunada¹ and Mikko Möttönen^{1,2}

1 QCD Labs, QTF Centre of Excellence, Department of Applied Physics, Aalto University, P.O. Box 15100, FI-00076 Aalto, Finland

2 QTF Centre of Excellence, VTT Technical Research Centre of Finland Ltd., P.O. Box 1000, 02044 VTT, Finland

* vasilii.1.vadimov@aalto.fi

Abstract

In circuit quantum electrodynamics systems, the quasiparticle-related losses in Josephson junctions are suppressed due to the gap in the superconducting density of states which is much higher than the typical energy of a microwave photon. In this work, we show that a strong drive even at frequency lower than the double superconducting gap enables dissipation in the junctions due to photon-assisted breaking of the Cooper pairs. Both the decay rate and noise strength associated with the losses are sensitive to the dc phase bias of the junction and can be tuned in a broad range by the amplitude and the frequency of the external driving field, making the suggested mechanism potentially attractive for designing tunable dissipative elements. Furthermore, pronounced memory effects in the driven Josephson junctions render them perspective for both theoretical and experimental study of non-Markovian physics in superconducting quantum circuits. We illustrate our theoretical findings by studying the spectral properties and the steady state population of a low impedance resonator coupled to the driven Josephson junction.

Copyright attribution to authors.

This work is a submission to SciPost Physics.

License information to appear upon publication.

Publication information to appear upon publication.

Received Date

Accepted Date

Published Date

Contents

1	Introduction	2
2	Model	3
2.1	Polarization operator	4
2.2	Quasiclassical limit	6
3	Admittance of the junction	7
3.1	Admittance of a static junction	8
3.2	Admittance of a driven junction	9
4	Low-impedance resonator	10
4.1	Spectroscopy of the driven resonator	12
4.2	Steady state population	13

5	Conclusions	14
A	Integration over the fermionic degrees of freedom	15
B	Stochastic unraveling	17
C	Transmission coefficient	17
D	Heat flow	18
	References	19

1 Introduction

Superconducting quantum circuits present one of the most versatile platforms for studying and utilizing macroscopic quantum phenomena [1–3]. Rapid development of experimental techniques and theoretical approaches has resulted in emergence of the research field of circuit quantum electrodynamics (cQED) [2–6]. The versatility of superconducting quantum devices allows for precise control of quantum state of the system [3, 7], study of dissipative quantum phase transitions [8–12], investigation of thermal phenomena [13–17], and development of microwave photonic metamaterials [6, 18–21]. Application-oriented research directions include microwave detectors [22–25], quantum sensing [26–28], and quantum computing [2, 4, 29–31], of which superconducting circuits are a leading hardware platform.

The key element of a superconducting quantum device is a Josephson junction [32, 33] which enables nonlinearity, or self-interaction, of the microwave photons in the circuit. In theoretical cQED, Josephson junctions are typically described as nonlinear inductors with a sinusoidal current-flux relation [3, 34]. However, it is known that the quasiparticle dynamics in the Josephson junctions leads to dissipation and memory effects [35, 36] which are not captured by this simple nonlinear inductor model. At millikelvin temperatures typical for superconducting quantum experiments, these effects are significant only at high frequencies above $\Delta_{\Sigma}/(2\pi\hbar)$ [37], where Δ_{Σ} is the sum of the superconducting gaps of the two leads; for commonly used aluminum-aluminum junctions this frequency is approximately 100 GHz. At the same time, the typical operational frequencies of the microwave field used in experiments have the order of 10 GHz or lower, which well justifies the use of the nonlinear inductor approximation. However, even in common superconducting devices, this approximation may be violated in the presence of a strong external microwave drive. The nonlinearity of the junction gives rise to frequency up-conversion, which may enable dissipation and memory effects even if the drive frequency is below $\Delta_{\Sigma}/(2\pi\hbar)$. Current trend of exploring higher frequency range (> 20 GHz) [38, 39] and high power drive [40, 41] calls for accurate theories which can capture effects of quasiparticles on the quantum dynamics of the microwave photons. Furthermore, theoretical and experimental study of the memory effects in a Josephson junction may be interesting from the point of view of non-Markovian open quantum system dynamics.

In addition to the fundamental values, study of the quasiparticle-induced losses in Josephson junctions gives prospects for development of tunable dissipative elements. In-situ control of dissipation strength can be utilized for unconditional on-demand reset of the quantum state of the system, which is one of the key operations in quantum computing [42]. Reset of superconducting qubits and resonators has been demonstrated [43–47] with a quantum circuit

refrigerator (QCR) [48–50], a device based on a voltage-biased double or a single [51] normal-metal–insulator–superconductor (NIS) junction. By changing the bias voltage, the same device can be used for preparation of hot thermal states [52] which enables operation of a quantum heat engine [53]. The dissipation induced by the QCR can also be controlled by rf drive [54,55] and by quasithermal noise [56] in the Brownian refrigerator regime [14,57]. The performance of QCR is typically limited by non-vanishing Dynes parameter of the superconducting lead and the temperature of the electrons in the normal lead, which results in reduced on/off ratio of the dissipation rate and imperfect cooling. These disadvantages are expected to be less restrictive in Josephson junctions, in which density of thermal quasiparticles is suppressed due to the spectral gap and the negligible subgap density of states in the superconducting leads enables one to completely turn off the dissipation. It has been shown that the dissipation in the Josephson junctions can be enabled by applying dc bias voltage [58–60]. In this work, we aim to explore the possibility of photonic cooling and heating with quasiparticle effects by driving a Josephson junction with a strong microwave signal.

The rest of the paper is organized as follows: in Sec. 2, we start from the microscopic model of a Josephson junction in quantized microwave field and derive a polarization operator of the microwave field. The polarization operator plays the role of a kernel in the influence functional arising from the fermionic bath. It also provides the time-nonlocal current-phase relation of the junction and statistics of the noise via fluctuation-dissipation theorem (FDT). In Sec. 3, we linearize the quasiclassical expression for the current through the junction to calculate its admittance with respect to a weak external microwave probe signal. We consider two cases: a non-driven phase-biased Josephson junction and a junction under a strong monochromatic drive. We show that the admittance of the junction as a function of complex frequency has singularities at the real frequency axis and that the external drive multiplies these singularities shifting them by integer multiple of drive frequency. As a result, the junction acquires non-vanishing active response, which is a signature of multiphoton-assisted Cooper pair breaking. In Sec. 4, we use the results of the previous Sections to analyze the dynamics of the microwave field in an LC -circuit shunted by a driven Josephson junction in the linear regime. First, we focus on the spectral properties of the LC -circuit and show the effect of the admittance singularities on the line shape of the resonator. Then, we analyze the steady state population of the LC -circuit and conclude that quasiparticle-enabled dissipation in the Josephson junction may result in both cooling and heating of the resonator, depending on the frequency and amplitude of the drive. Finally, we discuss our findings in Sec. 5.

2 Model

We start our analysis from a microscopic model of a Josephson junction in a quantized electromagnetic environment. Assuming the superconducting leads to be well described by the standard mean-field BCS model [61], we write the microscopic Hamiltonian for both electronic and electromagnetic degrees of freedom [62] as

$$\hat{H} = \hat{H}_{\text{EM}} + \sum_{\alpha k \sigma} \xi_{\alpha, k} \hat{c}_{\alpha, k \sigma}^\dagger \hat{c}_{\alpha, k \sigma} + \sum_{\alpha k} \left(\Delta_{\alpha} \hat{c}_{\alpha, k \uparrow}^\dagger \hat{c}_{\alpha, k \downarrow}^\dagger + h.c. \right) + \sum_{kk' \sigma} \frac{\gamma_{kk'}}{\sqrt{\mathcal{V}_l \mathcal{V}_r}} \left[\hat{c}_{l, k \sigma}^\dagger \hat{c}_{r, k' \sigma} e^{\frac{i\pi}{\Phi_0} (\hat{\phi}_l - \hat{\phi}_r)} + h.c. \right], \quad (1)$$

where \hat{H}_{EM} is the Hamiltonian of the electromagnetic degrees of freedom which contains fluxes and charges of the circuit nodes [63] and coupling to any external field, whose precise form is not relevant for our purposes. The index $\alpha = l, r$ denotes the left and right superconducting leads, respectively, the index k enumerates orbital electronic modes in the normal state, and

$\sigma = \uparrow, \downarrow$ stands for electron spin projection on a spin quantization axis. Energy of the normal electron in the state k in the lead α is given by $\xi_{\alpha,k}$, Δ_α is the superconducting gap in the corresponding lead, $\gamma_{kk'}$ is the tunneling matrix element between the modes k and k' of the two leads, \mathcal{V}_α is the volume of the lead α , $\hat{\phi}_\alpha$ is the flux operator of the lead α , and $\Phi_0 = \pi\hbar/e$ is the superconducting flux quantum. We assume that the orbital wavefunctions of the modes in the leads are symmetric with respect to time reversal, hence the tunneling matrix elements $\gamma_{kk'}$ are real. Without loss of generality we also assume the superconducting order parameters Δ_α to be real since the global phase can be transferred to the tunneling terms in the Hamiltonian by applying gauge transformation. Coupling between the electronic and electromagnetic degrees of freedom is provided by the tunneling operator $\hat{c}_{l,k\sigma}^\dagger \hat{c}_{r,k'\sigma} \exp(i\hat{\phi}/2) + h.c.$, where the phase of the tunneling matrix element is controlled by the phase difference operator as $\hat{\phi} = 2\pi(\hat{\phi}_l - \hat{\phi}_r)/\Phi_0$.

2.1 Polarization operator

We employ the path-integral approach presented in Refs. [64–66] generalized to the real time domain and integrate out the electronic degrees of freedom to obtain the time-nonlocal action for the phase difference across the junction (see Appendix A for the details). In the second order with respect to tunneling matrix element, the resulting Keldysh action reads as

$$S[\varphi^c, \varphi^q, \dots] = S_{\text{EM}}[\varphi^c, \varphi^q, \dots] + S_J[\varphi^c, \varphi^q]$$

$$S_J[\varphi^c, \varphi^q] = -\frac{1}{2} \left(\frac{\Phi_0}{2\pi} \right)^2 \int_{-\infty}^{+\infty} \boldsymbol{\chi}^\dagger(t) \begin{bmatrix} 0 & \boldsymbol{\Pi}^A(t-t') \\ \boldsymbol{\Pi}^R(t-t') & \boldsymbol{\Pi}^K(t-t') \end{bmatrix} \boldsymbol{\chi}(t') dt dt', \quad (2)$$

where φ^c and φ^q are so-called classical and quantum trajectories [67] of the phase difference across the junction, respectively, $S_{\text{EM}}[\varphi^c, \varphi^q, \dots]$ is the action of the electromagnetic environment originating from the Hamiltonian \hat{H}_{EM} , and $S_J[\varphi^c, \varphi^q]$ is the temporally non-local action of the junction arising from the path-integral over the electronic degrees of freedom. Here,

$$\boldsymbol{\chi}(t) = \begin{bmatrix} \boldsymbol{\chi}^c(t) \\ \boldsymbol{\chi}^q(t) \end{bmatrix}, \quad \boldsymbol{\chi}^c(t) = \begin{bmatrix} e^{\frac{i\varphi^c(t)}{2}} \cos \frac{\varphi^q(t)}{4} \\ e^{-\frac{i\varphi^c(t)}{2}} \cos \frac{\varphi^q(t)}{4} \end{bmatrix}, \quad \boldsymbol{\chi}^q(t) = \begin{bmatrix} ie^{\frac{i\varphi^c(t)}{2}} \sin \frac{\varphi^q(t)}{4} \\ -ie^{-\frac{i\varphi^c(t)}{2}} \sin \frac{\varphi^q(t)}{4} \end{bmatrix}, \quad (3)$$

and the 4×4 matrix-valued kernel in the junction action $S_J[\varphi^c, \varphi^q]$ is called the polarization operator. Fourier images of its retarded, advanced, and Keldysh 2×2 blocks components are given by

$$\boldsymbol{\Pi}^{\text{R/A/K}}(\omega) = \boldsymbol{\tau}_0 \boldsymbol{\Pi}_n^{\text{R/A/K}}(\omega) - \boldsymbol{\tau}_1 \boldsymbol{\Pi}_s^{\text{R/A/K}}(\omega), \quad (4)$$

where $\boldsymbol{\tau}_j$ for $j = 0, \dots, 3$ are the identity and Pauli matrices in Nambu space. Here, $\boldsymbol{\Pi}_n^{\text{R}}(\omega)$ and $\boldsymbol{\Pi}_s^{\text{R}}(\omega)$ stand for polarization operator components arising from normal and anomalous Green's functions of the leads, respectively:

$$\boldsymbol{\Pi}_n^{\text{R/A}}(\omega) = -\frac{i}{R_J} \int_{-\infty}^{+\infty} \left[g_l^{\text{R/A}}(\omega') g_r^{\text{K}}(\omega' - \omega) + g_l^{\text{K}}(\omega') g_r^{\text{A/R}}(\omega' - \omega) \right] d\omega',$$

$$\boldsymbol{\Pi}_s^{\text{R/A}}(\omega) = -\frac{i}{R_J} \int_{-\infty}^{+\infty} \left[f_l^{\text{R/A}}(\omega') f_r^{\text{K}}(\omega' - \omega) + f_l^{\text{K}}(\omega') f_r^{\text{A/R}}(\omega' - \omega) \right] d\omega', \quad (5)$$

$$\boldsymbol{\Pi}_{n/s}^{\text{K}}(\omega) = \left[\boldsymbol{\Pi}_{n/s}^{\text{R}}(\omega) - \boldsymbol{\Pi}_{n/s}^{\text{A}}(\omega) \right] \coth \left(\frac{\hbar\omega}{2k_B T_s} \right),$$

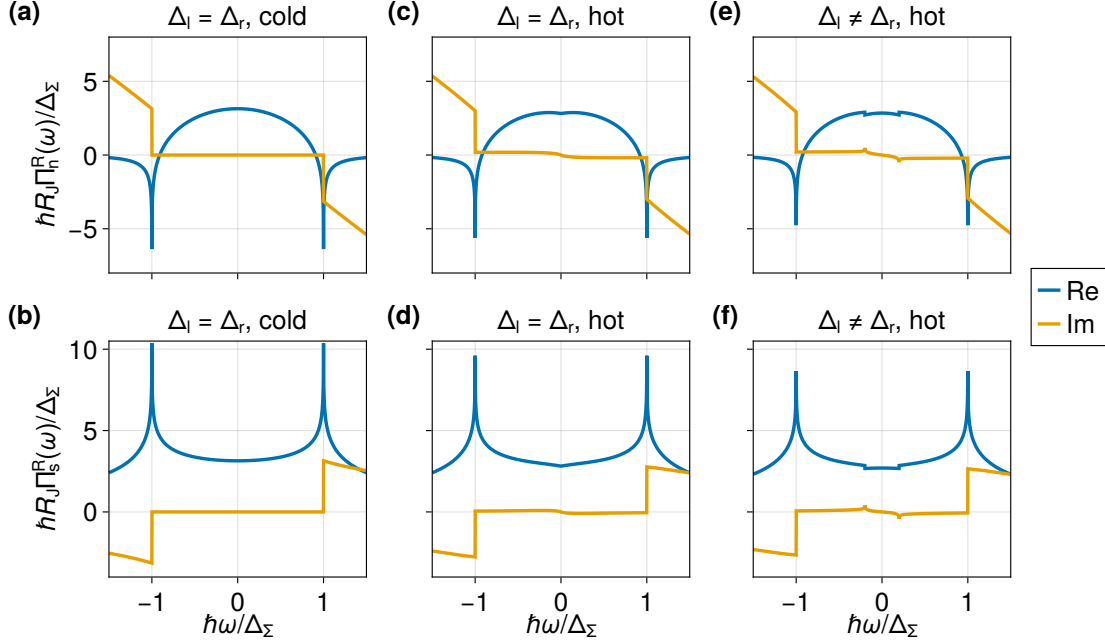


Figure 1: Retarded components of the polarization operator (a, c, e) $\Pi_n^R(\omega)$ and (b, d, f) $\Pi_s^R(\omega)$ as functions of frequency for (a, b) cold $k_B T_s = 0.04\Delta_\Sigma$ and (c, d, e, f) hot $k_B T_s = 0.32\Delta_\Sigma$ junctions. Here, (a, b, c, d) $\Delta_l = \Delta_r$, (e, f) $\Delta_l = 1.5 \times \Delta_r$, and $\nu_l = \nu_r = 0$.

where $R_J = (4\pi e^2 \gamma^2 N_l N_r)^{-1} \hbar$ is the tunneling resistance of the Junction in its normal state, T_s is the temperature of the electrons in the superconducting leads, and

$$g_\alpha^{R/A}(\omega) = -\frac{\hbar(\omega \pm i\nu_\alpha)}{\sqrt{\Delta_\alpha^2 - \hbar^2(\omega \pm i\nu_\alpha)^2}}, \quad f_\alpha^{R/A}(\omega) = -\frac{\Delta_\alpha}{\sqrt{\Delta_\alpha^2 - \hbar^2(\omega \pm i\nu_\alpha)^2}}, \quad (6)$$

$$g_\alpha^K(\omega) = [g_\alpha^R(\omega) - g_\alpha^A(\omega)] \tanh\left(\frac{\hbar\omega}{2k_B T_s}\right), \quad f_\alpha^K(\omega) = [f_\alpha^R(\omega) - f_\alpha^A(\omega)] \tanh\left(\frac{\hbar\omega}{2k_B T_s}\right).$$

are the retarded, advanced, and Keldysh components of the normal and anomalous quasiclassical Green's functions of the superconducting leads [61], and $\hbar\nu_\alpha/\Delta_\alpha$ is the Dynes parameter of the superconducting lead α . As we will see in the next subsection, the polarization operators $\Pi_n^R(\omega)$ and $\Pi_s^R(\omega)$ correspond to current-phase response functions for normal current and supercurrent, respectively.

In Fig. 1 we show the frequency dependence of the retarded polarization operators $\Pi_n^R(\omega)$ and $\Pi_s^R(\omega)$ for a symmetric junction $\Delta_l = \Delta_r$ in the cases of low temperature $k_B T_s \ll \Delta_\Sigma = \Delta_l + \Delta_r$ and relatively high temperature $k_B T_s \lesssim \Delta_\Sigma$ of the leads. The real and imaginary parts of the polarization operators are responsible for reactive and dissipative response, respectively. Due to retarded causality, they obey Kramers–Kronig relations [68]. We observe sharp logarithmic singularities of the polarization operator at frequencies $\omega = \pm\Delta_\Sigma/\hbar$ and emergence of strong dissipation at higher frequencies. This happens because the energy of a photon at such a high frequency is sufficient to break a Cooper pair and create two quasiparticles, one at each of the leads. In the case of a hot junction with a non-vanishing density of thermal quasiparticles, we also observe a weak $\omega \ln \omega$ -type singularity at zero frequency. Such a singularity corresponds to the tunneling of thermal quasiparticles [69, 70]. In the case of an asymmetric junction $\Delta_l \neq \Delta_r$ the corresponding singularity splits into two logarithmic singularities at frequencies

$\omega = \pm(\Delta_l - \Delta_r)/\hbar$ [71, 72], because the lowest energy quasiparticles need to acquire energy $|\Delta_l - \Delta_r|$ in order to tunnel to the other lead.

So far, we have considered a vanishing Dynes parameter, $\nu_\alpha = 0$. In the case of $\nu_\alpha > 0$, the logarithmic singularities of the polarization operators $\Pi_{n/s}^R(\omega)$ acquire an imaginary part on the order of $-i(\nu_l + \nu_r)$, which broadens the sharp features of the polarization operator at the real frequencies. In time domain, this corresponds to the exponential decay of $\Pi_{n/s}^R(t)$ on the time scale of $(\nu_l + \nu_r)^{-1}$. In the rest of the paper, we assume $\nu_\alpha = 0$ and provide qualitative reasoning for the case of non-vanishing Dynes parameters. We also restrict our analysis to the case of a symmetric junction $\Delta_l = \Delta_r$, for simplicity.

2.2 Quasiclassical limit

To clarify the physical meaning of the polarization operator, we explore the quasiclassical limit of the junction dynamics. To do so, we employ stochastic unraveling by applying Hubbard–Stratonovich transformation [67, 73, 74] to the terms of the action (2) which include Keldysh component of polarization operator [75] (see details in Appendix B):

$$\exp\left(\frac{i}{\hbar}S_J[\varphi^c, \varphi^q]\right) = \int \mathcal{D}[\xi, \xi^*] W[\xi, \xi^*] \exp\left(\frac{i}{\hbar}\tilde{S}_J[\varphi^c, \varphi^q, \xi, \xi^*]\right), \quad (7)$$

where $W[\xi, \xi^*]$ is the measure functional, which defines complex-valued Gaussian noise $\xi(t)$ with two-point correlation functions

$$\langle \xi^*(t)\xi(t') \rangle = i\hbar\Pi_n^K(t-t'), \quad \langle \xi(t)\xi(t') \rangle = -i\hbar\Pi_s^K(t-t'), \quad (8)$$

and noise action is given by

$$\begin{aligned} \tilde{S}_J[\varphi^c, \varphi^q, \xi, \xi^*] = & -\left(\frac{\Phi_0}{2\pi}\right)^2 \int_{-\infty}^{+\infty} \chi^{q\dagger}(t)\Pi^R(t-t')\chi^c(t') dt dt' \\ & + \frac{\Phi_0}{2\pi} \int_{-\infty}^{+\infty} [\xi^\dagger(t)\chi^q(t) + c.c.] dt. \end{aligned} \quad (9)$$

This action governs the dissipative dynamics of the phase degree of freedom explicitly driven by the shot noise. In the classical limit, the current through the junction is given by first variation of this action over the quantum phase:

$$I_J(t) = \frac{2\pi}{\Phi_0} \frac{\delta \tilde{S}_J[\varphi^c, \varphi^q, \xi, \xi^*]}{\delta \varphi^q(t)} = \langle I_J(t) \rangle + \tilde{I}_J(t). \quad (10)$$

The mean and the fluctuating part of the current read as

$$\begin{aligned} \langle I_J(t) \rangle = & \frac{\Phi_0}{4\pi} \int_{-\infty}^t \left\{ \Pi_s^R(t-t') \sin\left[\frac{\varphi^c(t) + \varphi^c(t')}{2}\right] - \Pi_n^R(t-t') \sin\left[\frac{\varphi^c(t) - \varphi^c(t')}{2}\right] \right\} dt', \\ \tilde{I}_J(t) = & \frac{i\xi^*(t)}{4} \exp\left[\frac{i\varphi^c(t)}{2}\right] - \frac{i\xi(t)}{4} \exp\left[-\frac{i\varphi^c(t)}{2}\right], \end{aligned} \quad (11)$$

respectively.

We can make two important remarks about Eq. (11). First, the current is not an instantaneous function of the time-dependent phase difference, but also depends on its past. The

retarded components of the polarization operators $\Pi_n^R(\omega)$ and $\Pi_s^R(\omega)$ play the role of kernels for two components of the current: the one which is invariant with respect to a global constant in time shift of the phase difference, and the one which is not. Therefore, we can conclude that these polarization operators play the role of current-phase response functions for normal current and supercurrent, respectively. The second remark is that the current through the junction is noisy. The noise statistics is determined by the Keldysh components $\Pi_n^K(\omega)$ and $\Pi_s^K(\omega)$ with the latter controlling the phase of the noise. The noise spectral density is related to the retarded response function via the fluctuation-dissipation theorem (5). Due to the zero-frequency pole of $\coth[\hbar\omega/(2k_B T_s)]$, the noise spectral density of a hot symmetric junction has a logarithmic singularity. In time domain, this results in a slow $1/|t-t'|$ asymptotic decay of noise correlation function, which is detrimental for the phase coherence.

In the low temperature limit with no quasiparticles, the polarization operators in time domain are fast oscillating functions of time with the frequency of oscillations given by Δ_Σ/\hbar . If the dynamics of the phase is slow, these fast oscillations are irrelevant and the adiabatic approximation $\Pi_{n/s}^R(t-t') \propto \delta(t-t')$ can be employed. Under this assumption, we recover the standard time-local current-phase relation [34]

$$I_J(t) = \frac{\Phi_0}{2\pi} \Pi_s^R(\omega)|_{\omega=0} \sin[\varphi^c(t)], \quad (12)$$

which means that the adiabatic approximation yields the nonlinear inductor model of the Josephson junction. This relation allows us to obtain the Josephson energy as

$$E_J = \frac{1}{2} \left(\frac{\Phi_0}{2\pi} \right)^2 \Pi_s^R(\omega)|_{\omega=0}. \quad (13)$$

For a symmetric junction $\Delta_l = \Delta_r = \Delta$ with vanishing Dynes parameters $\nu_l = \nu_r = 0$, we recover the standard Ambegaokar–Baratoff formula for the Josephson energy [76]

$$E_J = \frac{R_Q}{2R_J} \Delta \tanh\left(\frac{\Delta}{2k_B T_s}\right), \quad (14)$$

where $R_Q = 2\pi\hbar/(2e)^2 \approx 6.45 \text{ k}\Omega$ is the resistance quantum.

In the following Sections, we explore regimes when the adiabatic approximation for the current-phase relation breaks down. As we argued above, this can be achieved by applying a strong microwave drive. The nonlinearity of the junction can up-convert the drive frequency above Δ_Σ/\hbar , which is sufficient for observation of the memory effects. In the rest of the paper, we fully rely on the quasiclassical approximation and neglect all the quantum effects except the Bose–Einstein statistics of the photons. This is justified in the limit of small quantum fluctuations of the phase which is controlled by the impedance of the electromagnetic environment of the junction [51, 58, 59, 62].

3 Admittance of the junction

In this section, we analyze the admittance of the junction in equilibrium and under the external drive. We assume that the junction is biased to have a dc phase difference φ_0 and driven monochromatically by voltage $V_d(t) = V_0 \cos(\Omega t)$. By admittance we consider the linear response of the current with respect to a weak probe voltage $v_p(t)$ which is applied in addition to the monochromatic drive. To obtain it, we find that the total phase difference across the junction is given by

$$\varphi(t) = \varphi_d(t) + \frac{2e}{\hbar} \int^t v_p(t') dt', \quad (15)$$

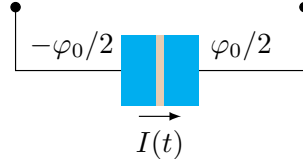
$$V(t) = V_0 \cos(\Omega t) + v_p(t)$$


Figure 2: Monochromatic drive and weak probe voltage applied to a phase-biased Josephson junction.

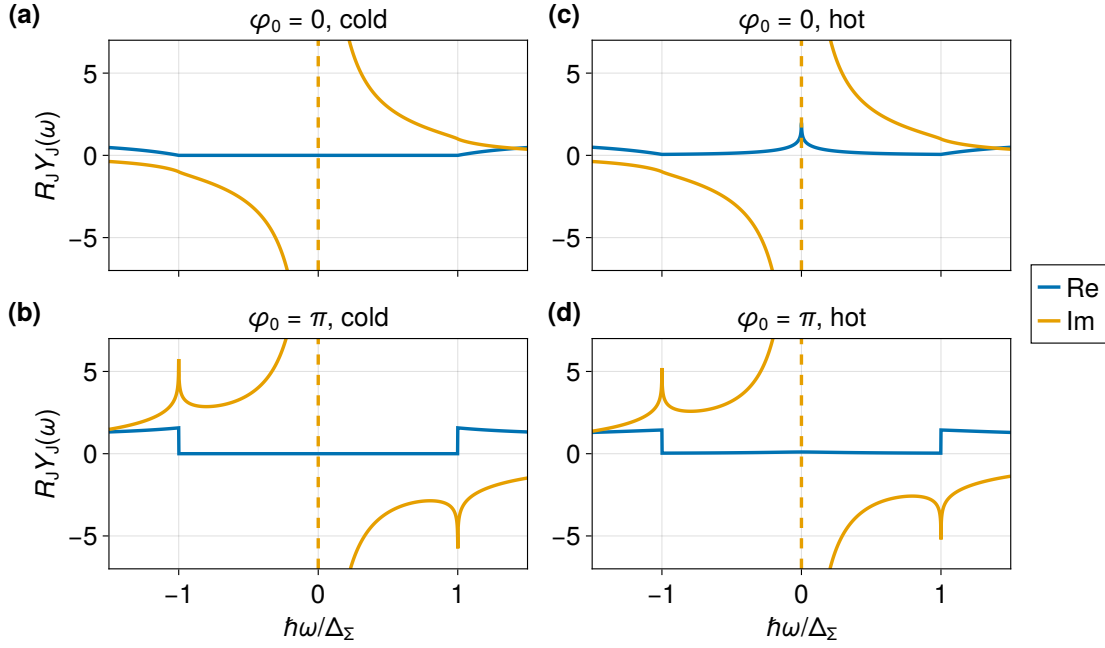


Figure 3: Admittance of a static symmetric Josephson junction. The temperature of the superconducting leads is (a, b) $k_B T_s = 0.04 \Delta_\Sigma$, (c, d) $k_B T_s = 0.32 \Delta_\Sigma$.

where we have omitted the superscript “c” for brevity and explicitly separated the weak probe voltage $v_p(t)$ from the sum of the dc phase bias and the phase coming from the drive

$$\varphi_d(t) = \varphi_0 + \frac{2eV_0}{\hbar\Omega} \sin(\Omega t). \quad (16)$$

To obtain the admittance, we linearize Eq. (11) with respect to $v_p(t)$ and omit the noise terms.

3.1 Admittance of a static junction

First, we analyze a simpler case of absent drive $V_0 = 0$. In this case, the current is given by

$$\langle I_J(t) \rangle = \frac{\Phi_0}{4\pi} \Pi_s^R(\omega) \Big|_{\omega=0} \sin \varphi_0 + \int_{-\infty}^t Y_J(t-t'; \varphi_0) v_p(t') dt'. \quad (17)$$

The first term corresponds to the dc Josephson current. The Fourier image of the admittance reads as

$$Y_J(\omega; \varphi_0) = \frac{i}{\omega} \left[\tilde{\Pi}_n^R(\omega, 0) + \tilde{\Pi}_s^R(\omega, 0) \cos \varphi_0 \right], \quad (18)$$

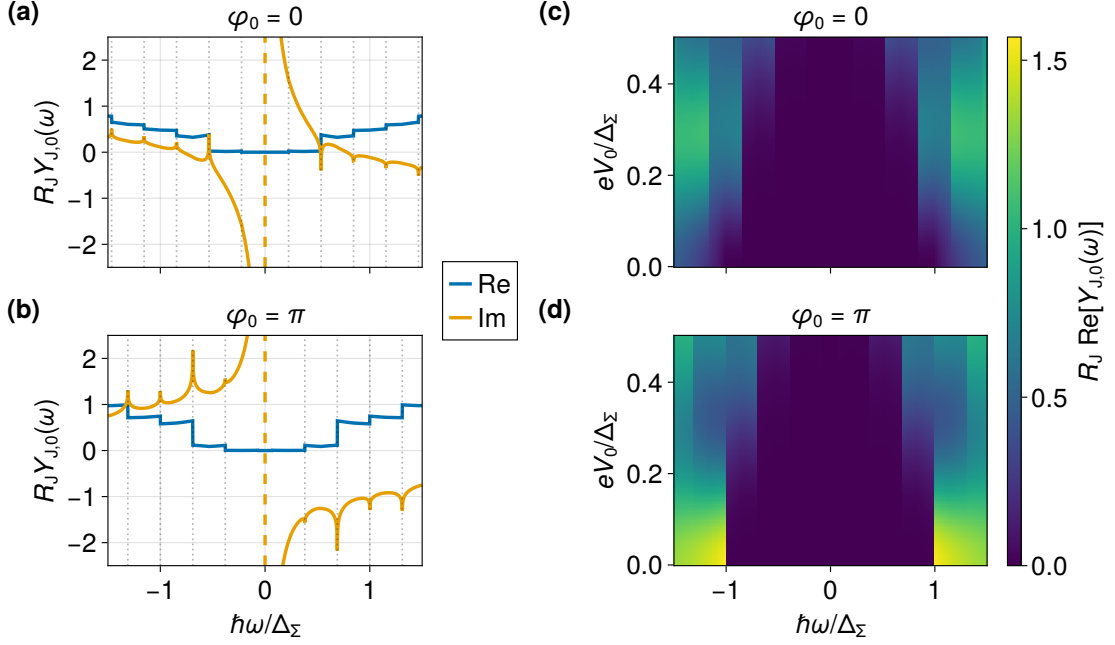


Figure 4: Frequency-preserving admittance component $Y_{J,0}(\omega)$ of a driven symmetric Josephson junction. The temperature of the superconducting leads is $k_B T_s = 0.04\Delta_\Sigma$, drive frequency is $\hbar\Omega = 0.155\Delta_\Sigma$. (a, b) Real and imaginary components of the admittance for the drive amplitude $eV_0 = 0.5\Delta_\Sigma$. The vertical black dotted lines highlight logarithmic singularities of the admittance at frequencies $\omega = \pm\Delta_\Sigma/\hbar + n\Omega$, where n is (a) odd (b) even integer number. (c, d) Real component of admittance as a function of frequency and drive amplitude.

where we have introduced shorthand notations

$$\tilde{\Pi}_n^R(\omega, \omega') = \frac{\Pi_n^R(\omega + \omega') - \Pi_n^R(\omega')}{4}, \quad \tilde{\Pi}_s^R(\omega, \omega') = \frac{\Pi_s^R(\omega + \omega') + \Pi_s^R(\omega')}{4}. \quad (19)$$

In Fig. 3 we show the frequency dependence of the junction admittance for $\varphi_0 = 0$ and $\varphi_0 = \pi$. In the former case, we clearly see a $1/\omega$ divergence of the imaginary part of the admittance, which corresponds to the standard inductive response of a Josephson junction at low frequencies. For the cold junction, the dissipation is suppressed in the range of frequencies $\hbar|\omega| < \Delta_\Sigma$. This is not the case for the hot junction, where the thermal quasiparticles lead to emergence of a logarithmic singularity in the real part of the admittance. For the junction biased to $\varphi_0 = \pi$, the inductive component of the response flips its sign as expected. The dissipation at high frequencies $\hbar|\omega| > \Delta_\Sigma$ turns out to be significantly stronger than in the unbiased case $\varphi_0 = 0$, which means that Cooper pair breaking happens more efficiently. However, the real part of the low frequency admittance of the hot π -biased junction is strongly suppressed compared to the unbiased one, which is explained by the coherent suppression of quasiparticle tunneling [77, 78]. At arbitrary phase bias φ_0 , neither the Cooper pair breaking nor quasiparticle tunneling is suppressed, so we have uncompensated dissipation at both high and low frequencies.

3.2 Admittance of a driven junction

Now we proceed to the case of a non-vanishing drive at frequency Ω . The noiseless part of the current (11) linearized with respect to the probe voltage is given by

$$\begin{aligned} \langle I_J(t) \rangle = & \frac{\Phi_0}{4\pi} \text{Im} \sum_{n,n'=-\infty}^{\infty} c_{n'} e^{-in\Omega t} [c_{n-n'} \tilde{\Pi}_s^R(n'\Omega) + c_{n'-n}^* \tilde{\Pi}_n^R(n'\Omega)] \\ & + \sum_{n=-\infty}^{\infty} e^{-in\Omega t} \int_{-\infty}^t Y_{J,n}(t-t'; \varphi_0, V_0, \Omega) v_p(t') dt'. \end{aligned} \quad (20)$$

Here, we have introduced the Fourier coefficients

$$c_n = \frac{\Omega}{2\pi} \int_0^{2\pi/\Omega} e^{in\Omega t + \frac{i\varphi_d(t)}{2}} dt = e^{\frac{i\varphi_0}{2}} J_n\left(-\frac{eV_0}{\hbar\Omega}\right), \quad (21)$$

where $J_n(x)$ is the n -th Bessel function. The first sum in Eq. (20) describes the current due to the drive in the absence of probe signal. The response to the probe tone at frequency ω_p contains frequencies $\omega_p + n\Omega$ for every integer n due to the nonlinear frequency mixing in the junction. Thus, each frequency shift $n\Omega$ has a corresponding admittance:

$$Y_{J,n}(\omega; \varphi_0, V_0, \Omega) = \frac{i}{2\omega} \sum_{n'=-\infty}^{+\infty} [c_{n'-n}^* \quad c_{n-n'}] \begin{bmatrix} \tilde{\Pi}_n^R(\omega, n'\Omega) & \tilde{\Pi}_s^R(\omega, n'\Omega) \\ \tilde{\Pi}_s^R(\omega, n'\Omega) & \tilde{\Pi}_n^R(\omega, n'\Omega) \end{bmatrix} \begin{bmatrix} c_{n'} \\ c_{-n'}^* \end{bmatrix} \quad (22)$$

The plots of the frequency-preserving component of the admittance $Y_{J,0}(\omega; \varphi_0, V_0, \Omega)$ are shown in Fig. 4. First, we observe that the residue of the inductive pole at zero frequency has changed, which is a manifestation of the ac-Stark effect. We also clearly see that frequency mixing gives rise to multiple singularities located at frequencies $\omega = \pm\Delta_{\Sigma}/\hbar + n\Omega$. Each of these singularities corresponds to enabling or disabling of a Cooper pair breaking process involving n photons from the drive and a single photon from the probe: Cooper pair breaking with absorption of n photons from the drive and absorption or emission of a single probe photon at frequency ω is allowed if $n\Omega > \Delta_{\Sigma}/\hbar \mp \omega$, respectively. We also notice that the character of the singularities depends on the dc phase bias: for the unbiased and π -biased junction the Cooper pair breaking is more efficient for processes involving odd and even number of drive photons, respectively.

The highly non-trivial dependence of the admittance on the probe frequency may result in complex dynamics of the electromagnetic field in the superconducting circuits and memory effects. The latter should be especially well pronounced if a normal mode of the circuit has a frequency close to the singularity of the admittance. Another important effect is that the balance between the photon-absorption and photon-emission processes involving different numbers of drive photons determines the population of the normal modes in the steady state. Such a phenomenon can be used in applications for cooling and heating the photonic system. In the following Section, we confirm this qualitative reasoning with direct calculations for a simple example of an LC -circuit shunted with a driven Josephson junction.

4 Low-impedance resonator

We consider a circuit shown in Fig. 5 shunted with a Josephson junction to the ground through an ideal voltage source. The junction is biased by an external flux and the resonator is probed through a capacitively coupled transmission line. We assume the coupling capacitance C_p to be infinitesimally small, so the dissipation induced by the probe is negligible relative to the one induced by the junction. We consider the limit of a low-impedance circuit, where the characteristic impedance $Z_r = \sqrt{L_r/C_r}$ meets the condition $Z_r \ll R_Q$ and the Josephson inductance is much higher than the intrinsic inductance of the resonator $\Phi_0^2/E_J \gg L_r$. These assumptions

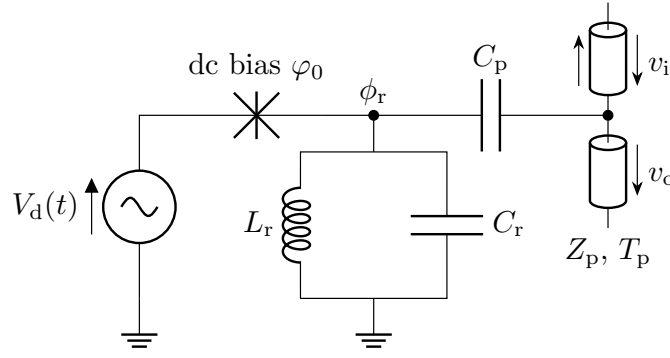


Figure 5: Schematic of a circuit. An LC circuit is driven through a Josephson junction and probed through a capacitively coupled transmission line.

Table 1: Parameters of the circuit presented in Fig. 5, used for calculations.

C_r	L_r	Δ_l	Δ_r	R_J	T_s
637 fF	1.59 nH	0.2 meV	0.2 meV	30 k Ω	0.2 K

allow us to neglect any nonlinear effects in the dynamics of the LC -circuit induced by the junction [51, 58, 59]. We also assume that the drive frequency of the junction is highly off-resonant $\Omega \gg \omega_r = 1/\sqrt{L_r C_r}$. This condition allows us to neglect the off-resonant Josephson current related to the driving field as well as frequency conversion of the microwave field in the resonator. Thus, the dynamics of the resonator flux degree of freedom ϕ_r is governed by the following equation:

$$C_r \ddot{\phi}_r(t) + \int_{-\infty}^t Y_{J,0}(t-t'; \varphi_0, V_0, \Omega) \dot{\phi}_r(t') dt' + \frac{\phi_r(t)}{L_r} = -\tilde{I}_J(t; \varphi_0, V_0, \Omega), \quad (23)$$

$$\tilde{I}_J(t; \varphi_0, V_0, \Omega) = \frac{i\xi^*(t)}{4} \exp\left[\frac{i\varphi_d(t)}{2}\right] - \frac{i\xi(t)}{4} \exp\left[-\frac{i\varphi_d(t)}{2}\right].$$

Here, we assume that the noise component of the current (see Eq. (11)) is not affected by the flux degree of freedom ϕ_r of the LC -circuit but only by the external drive (16). The solution of this equation can be expressed through the retarded Green's function of the resonator:

$$\phi_r(t) = \int_{-\infty}^t G_{r,0}^R(t-t'; \varphi_0, V_0, \Omega) \tilde{I}_J(t'; \varphi_0, V_0, \Omega) dt', \quad (24)$$

Fourier image of which is given by

$$G_{r,0}^R(\omega; \varphi_0, V_0, \Omega) = \frac{L_r}{\omega^2 L_r C_r + i\omega L_r Y_{J,0}(\omega; \varphi_0, V_0, \Omega) - 1}. \quad (25)$$

We also define the Keldysh Green's function of the LC -circuit as a flux-flux correlator

$$G_r^K(t, t'; \varphi_0, V_0, \Omega) = -\frac{i}{\hbar} \langle \phi_r(t) \phi_r(t') \rangle = \sum_{n=-\infty}^{+\infty} e^{-in\Omega t} G_{r,n}^K(t-t'; \varphi_0, V_0, \Omega), \quad (26)$$

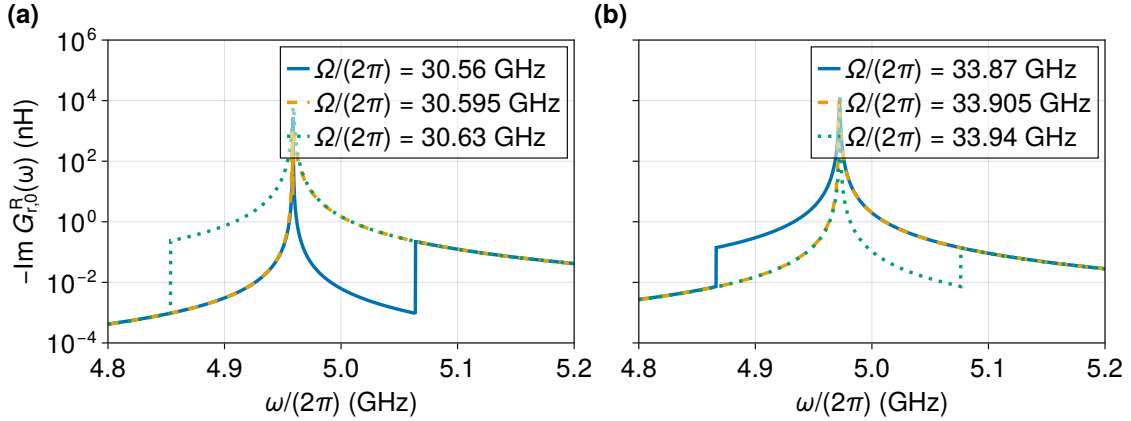


Figure 6: Imaginary part of the Green's function $G_{r,0}^R(\omega)$ for three different frequencies Ω in the vicinity of (a) $\tilde{\omega}_r + 3\Omega \approx \Delta_\Sigma/\hbar$, corresponding to photon-assisted Cooper pair breaking with absorption of three drive photons and single photon from the resonator, and (b) $-\tilde{\omega}_r + 3\Omega \approx \Delta_\Sigma/\hbar$ resonances, corresponding to absorption of three drive photons and emission of a single photon to the resonator. Here, the parameters of the circuit are taken from Tab. 1, the phase bias is $\varphi_0 = 0$, and the drive amplitude is equal to $V_0 = 0.2$ mV.

where $G_{r,n}^K(t - t'; \varphi_0, V_0, \Omega)$ are defined through their Fourier images

$$G_{r,n}^K(\omega; \varphi_0, V_0, \Omega) = \frac{1}{16} G_{r,0}^R(\omega + n\Omega; \varphi_0, V_0, \Omega) G_{r,0}^A(\omega; \varphi_0, V_0, \Omega) \times \sum_{n'=-\infty}^{\infty} [c_{n'-n}^* \quad c_{n-n'}] \tau_3 \Pi^K(\omega + n'\Omega) \tau_3 \begin{bmatrix} c_{n'} \\ c_{-n'}^* \end{bmatrix}. \quad (27)$$

and the advanced Green's function related to the retarded one as

$$G_{r,0}^A(\omega; \varphi_0, V_0, \Omega) = [G_{r,0}^R(\omega; \varphi_0, V_0, \Omega)]^*. \quad (28)$$

The spectral structure of the resonator is contained in its retarded Green's function, while the Keldysh component also has information on its steady-state population. In the following, we discuss experimentally observable quantities which can provide us information about the Green's functions.

4.1 Spectroscopy of the driven resonator

First, we start with an analysis of a single-tone spectroscopy of the resonator. We send a coherent tone at frequency ω to one of the ports shown in Fig. 5 and probe the transmitted field at the same frequency from the other port. In principle, frequency mixing gives rise to the response at $\omega + n\Omega$ for integer n , but we have neglected this effect by taking into account only the frequency-conserving component of the admittance. The transmission coefficient $S_{21}(\omega)$ can be expressed through the retarded component of the Green's function of the resonator. In the second order with respect to the coupling capacitance C_p , it reads as

$$S_{21}(\omega) \approx 1 + \frac{i}{2} \omega Z_p C_p - \frac{1}{4} (\omega Z_p C_p)^2 - \frac{i}{2} \omega^3 Z_p C_p^2 G_{r,0}^R(\omega). \quad (29)$$

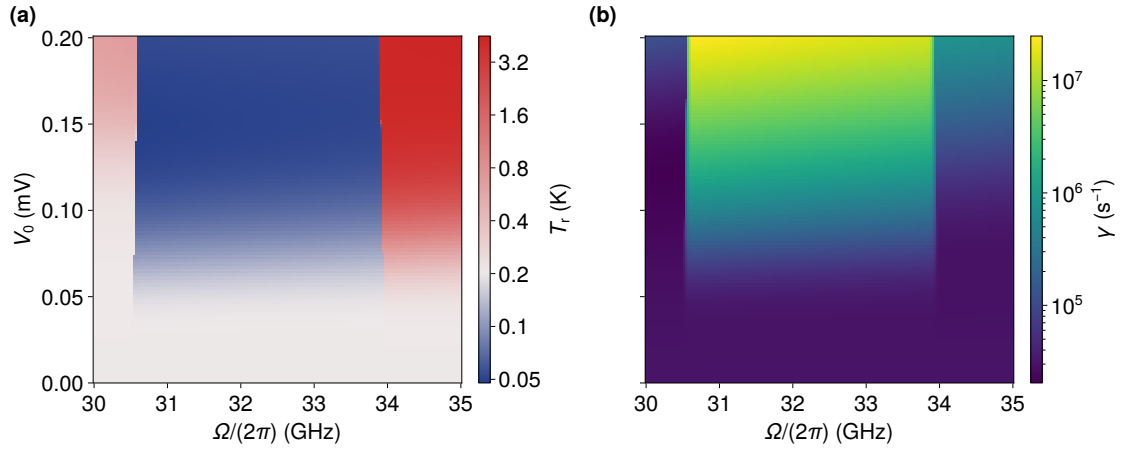


Figure 7: (a) Quasitemperature of the resonator as a function of the frequency and amplitude of the drive. The red color represents a higher temperature compared to the temperature of the Josephson junction, and the blue color represents a lower one. (b) Dependence of the resonator decay rate on the drive frequency and amplitude for the phase bias $\varphi_0 = 0$.

The derivation can be found in Appendix C. In the lowest order with respect to the coupling, the contribution to the absolute value of the transmission coefficient $|S_{21}(\omega)|^2$ is given by the imaginary part of the retarded Green's function of the resonator. In Fig. 6 we show the plots of $\text{Im} G_{r,0}^R(\omega)$ for different drive frequencies. We observe that, if the ac-Stark-shifted LC -circuit frequency is resonant with the singularity of the junction admittance, the line shape of the LC -circuit deviates from a Lorentzian, which results in non-exponential decay and, consequently, non-Markovian dynamics of the electromagnetic field in the circuit. The sharpness of the non-Lorentzian feature is determined by the Dynes parameter. In the realistic case of $\nu_\alpha/\Delta_\alpha \sim 10^{-4}$, the broadening of the logarithmic singularities of the admittance can be of the order of ~ 10 MHz for an aluminum junction. This circumstance may hinder an experimental observation of the non-Lorentzian spectrum of the resonator, especially if the decay rate due to the Cooper pair breaking is lower than this broadening.

In addition to the non-Lorentzian feature, we see that the linewidth of the resonator differs significantly for drive frequencies on different sides of the resonance. This opens a possibility to use driven Josephson junctions as tunable dissipative elements similarly to NIS-junction based QCRs [48–50].

4.2 Steady state population

Since the rate of photon-assisted Cooper pair breaking processes which involve absorption or emission of the resonator photons strongly depends on the drive parameters, a driven Josephson junction may effectively cool or heat the LC -circuit. However, the distribution of the photons is in principle not thermal and cannot be described with a single well-defined temperature. To quantify the population of incoherent photons in the resonator, we assume that the probe line has a well-defined temperature T_p . Then, we can calculate the heat flow from probe line to the resonator averaged the noise realizations and in time over the drive period $\langle W(T_p) \rangle$. In the lowest order with respect to the coupling capacitance, it is given by

$$\langle W(T_p) \rangle \approx \hbar \frac{C_p^2 Z_p}{2} \int_{-\infty}^{+\infty} \text{Im} \left[G_{r,0}^K(\omega) - G_{r,0}^R(\omega) \coth \left(\frac{\hbar\omega}{2k_B T_p} \right) \right] \frac{\omega^4 d\omega}{2\pi}. \quad (30)$$

The details of the derivation of the heat flow power are presented in Appendix D. If the resonator were in the true thermal equilibrium with temperature T_r , the heat flow would vanish in the case of equal temperatures $T_r = T_p$. Therefore, we can assign a quasitemperature T_r to the resonator as the temperature of the probe which corresponds to the vanishing of the heat flow, i.e. $\langle \overline{W(T_r)} \rangle = 0$.

We present the plots of the steady-state quasitemperature and linewidth of the resonator vs. the drive frequency and amplitude in Fig. 7. One can clearly observe both of these quantities change sharply at the resonances which correspond to the Cooper pair breaking. The frequencies of the resonances depend on the amplitude because of the ac-Stark shift of the resonator. The steady-state quasitemperature is determined by the dominant process of Cooper pair breaking. The regions of the parameter space where the photon absorption from the resonator dominates correspond to cooling of the circuit. In the other regions, the Cooper pair breaking with photon emission is stronger, and the resonator heats up.

Based on our results, we conclude that the driven Josephson junctions can serve as tunable dissipative elements. Both the quasitemperature and the decay rate can be efficiently tuned in a broad range, which makes this dissipation mechanism potentially interesting for such practical applications as unconditional ground state preparation [43] or implementation of a quantum heat engine [53]. However, this work serves merely as a proof of principle, and we leave optimization of the drive parameters and analysis of the effects of non-vanishing Dynes parameter and elevated electronic temperature for future studies.

5 Conclusions

We analyzed the effects of memory and dissipation in a strongly-driven Josephson junction on the dynamics of the electromagnetic field in cQED systems within the quasiclassical approximation. At low temperature, the mechanism responsible for both of these effects is photon-assisted Cooper pair breaking. Despite the fact that breaking a Cooper pair in a Josephson junction requires an energy much higher than the typical energies in cQED systems, multiphoton processes enabled by the junction nonlinearity make experimental observation of the dissipation and non-Markovian dynamics feasible. We illustrate this on a simple system of a linear LC -circuit coupled to a strongly driven Josephson junction; our findings include the emergence of a non-Lorentzian line shape in case of a resonance with one of the photon-assisted Cooper pair breaking channels and the control of resonator quasitemperature and decay rate by external drive.

Our theoretical approach, however, has certain limitations: we take into account the nonlinearity of the junction only with respect to the external classical drive and neglect the effect of quantum fluctuations of the microwave field in the resonator. This makes our approach inapplicable to systems where either of these approximations is violated, e.g., qubits or Josephson junctions coupled to high-impedance linear resonators [59]. Analysis of nonlinear quantum non-Markovian dynamics of the system can be done using more advanced numerical methods, such as the hierarchical equation of motion [79–81] capable of accurate treatment of highly structured and low-temperature environments. However, the presented quasiclassical approach may still be helpful for qualitative analysis and estimates for a weakly nonlinear system such as a transmon qubit.

Acknowledgments

VV thanks Marko Kuzmanović, Ognjen Stanisavljević, Julien Basset, and Jérôme Estève for fruitful discussions. This work has been financially supported by the Academy of Finland Centre of Excellence program (Project No. 336810) and THEPOW (Project No. 349594), the European Research Council under Advanced Grant No. 101053801 (ConceptQ). We acknowledge the computational resources provided by the Aalto Science-IT project.

A Integration over the fermionic degrees of freedom

Action on a Keldysh contour corresponding to Hamiltonian (1) reads as [64, 67]

$$S[\bar{\mathbf{c}}, \mathbf{c}, \varphi^c, \varphi^q, \dots] = S_{\text{EM}}[\varphi^c, \varphi^q, \dots] + S_{\text{SIS}}[\bar{\mathbf{c}}, \mathbf{c}, \varphi^c, \varphi^q], \quad (31)$$

where $S_{\text{EM}}[\varphi^c, \varphi^q, \dots]$ is an action of electromagnetic environment of the junction and $S_{\text{SIS}}[\bar{\mathbf{c}}, \mathbf{c}, \varphi^c, \varphi^q]$ is the action of the Josephson junction in the electromagnetic environment:

$$S_{\text{SIS}}[\bar{\mathbf{c}}, \mathbf{c}, \varphi^c, \varphi^q] = \int_{-\infty}^{+\infty} \left\{ \sum_{\alpha, k} \bar{\mathbf{c}}_{\alpha, k}(t) \mathbf{G}_{\alpha, k}^{-1} \mathbf{c}_{\alpha, k}(t) - \sum_{kk'} \frac{\gamma_{kk'}}{\sqrt{\lambda_l \lambda_r}} \left[\bar{\mathbf{c}}_{l, k}(t) \mathbf{\Gamma}(\varphi^c(t), \varphi^q(t)) \mathbf{c}_{r, k'}(t) + \bar{\mathbf{c}}_{r, k'}(t) \mathbf{\Gamma}^\dagger(\varphi^c(t), \varphi^q(t)) \mathbf{c}_{l, k}(t) \right] \right\} dt. \quad (32)$$

Here,

$$\bar{\mathbf{c}}_{\alpha, k}(t) = \begin{bmatrix} \bar{c}_{\alpha, k\uparrow}^{(1)}(t) & c_{\alpha, k\downarrow}^{(1)}(t) & \bar{c}_{\alpha, k\uparrow}^{(2)}(t) & c_{\alpha, k\downarrow}^{(2)}(t) \end{bmatrix}, \quad \mathbf{c}_{\alpha, k}(t) = \begin{bmatrix} c_{\alpha, k\uparrow}^{(1)}(t) \\ \bar{c}_{\alpha, k\downarrow}^{(1)}(t) \\ c_{\alpha, k\uparrow}^{(2)}(t) \\ \bar{c}_{\alpha, k\downarrow}^{(2)}(t) \end{bmatrix} \quad (33)$$

are Grassmanian trajectories which describe electronic degrees of freedom combined for convenience in vectors in Keldysh–Nambu space, the inverse matrix-valued Green’s functions of electrons have block structure in Keldysh space

$$\mathbf{G}_{\alpha, k}^{-1} = \begin{bmatrix} \mathbf{0} & \left[\mathbf{G}_{\alpha, k}^{-1} \right]^{\text{A}} \\ \left[\mathbf{G}_{\alpha, k}^{-1} \right]^{\text{R}} & \left[\mathbf{G}_{\alpha, k}^{-1} \right]^{\text{K}} \end{bmatrix}, \quad (34)$$

where retarded, advanced, and Keldysh components of inverse Green’s function are given by

$$\left[\mathbf{G}_{\alpha, k}^{-1} \right]^{\text{R/A}} = i\hbar(\partial_t \pm \nu_\alpha) \boldsymbol{\tau}_0 - \xi_{\alpha, k} \boldsymbol{\tau}_3 - \Delta_\alpha \boldsymbol{\tau}_1, \quad \left[\mathbf{G}_{\alpha, k}^{-1} \right]^{\text{K}} = 2i\hbar \nu_\alpha \boldsymbol{\tau}_0 \tanh\left(\frac{i\hbar \partial_t}{2k_{\text{B}} T_s}\right), \quad (35)$$

$\hbar \nu_\alpha / \Delta_\alpha$ is the Dynes parameter of the superconducting lead α , $\boldsymbol{\tau}_j$, $j = 0, \dots, 3$ are Pauli matrices in Nambu space, and T_s is the temperature of the superconducting leads which is assumed to be common for both of them. The phase-dependent tunneling matrix is given by

$$\mathbf{\Gamma}(\varphi^c, \varphi^q) = \begin{bmatrix} i e^{i \frac{\varphi^c}{2} \boldsymbol{\tau}_3} \sin \frac{\varphi^q}{4} & \boldsymbol{\tau}_3 e^{i \frac{\varphi^c}{2} \boldsymbol{\tau}_3} \cos \frac{\varphi^q}{4} \\ \boldsymbol{\tau}_3 e^{i \frac{\varphi^c}{2} \boldsymbol{\tau}_3} \cos \frac{\varphi^q}{4} & i e^{i \frac{\varphi^c}{2} \boldsymbol{\tau}_3} \sin \frac{\varphi^q}{4} \end{bmatrix}. \quad (36)$$

To obtain the influence functional for the electromagnetic field, we need to evaluate Gaussian Grassmanian path integral

$$\exp\left(\frac{i}{\hbar}S_J[\varphi^c, \varphi^q]\right) = \int \mathcal{D}[\bar{\mathbf{c}}, \mathbf{c}] \exp\left(\frac{i}{\hbar}S_{\text{SIS}}[\bar{\mathbf{c}}, \mathbf{c}, \varphi^c, \varphi^q]\right). \quad (37)$$

For integral operators \mathbf{G}^{-1} and \mathbf{V} acting in time domain

$$(\mathbf{G}^{-1}\mathbf{f})(t) = \int_{-\infty}^{+\infty} \mathbf{G}^{-1}(t, t')\mathbf{f}(t') dt', \quad (\mathbf{V}\mathbf{f})(t) = \int_{-\infty}^{+\infty} \mathbf{V}(t, t')\mathbf{f}(t') dt', \quad (38)$$

where $\mathbf{f}(t)$ is a placeholder vector-valued function of time, the following relation holds for Grassmanian path integral:

$$\begin{aligned} \int \mathcal{D}[\bar{\mathbf{c}}, \mathbf{c}] \exp\left\{\frac{i}{\hbar} \int_{-\infty}^{+\infty} \bar{\mathbf{c}}(t)[(\mathbf{G}^{-1} - \mathbf{V})]\mathbf{c}(t) dt\right\} &= \exp\left\{\text{Tr} \log\left[\frac{i}{\hbar}(\mathbf{G}^{-1} - \mathbf{V})\right]\right\} \\ &= \det\left(\frac{i\mathbf{G}^{-1}}{\hbar}\right) \exp\left[\text{Tr} \sum_{n=1}^{\infty} \frac{(-1)^n}{n} (\mathbf{G}\mathbf{V})^n\right]. \end{aligned} \quad (39)$$

Here, \mathbf{G} is the inverse operator of \mathbf{G}^{-1} , the logarithm is to be understood as a function of an operator, and a trace of an operator with kernel $A(t, t')$ in time domain is given by

$$\text{Tr} \mathbf{A} = \int_{-\infty}^{+\infty} \text{Tr} \mathbf{A}(t, t) dt. \quad (40)$$

Applying this formula to Eq. (32) and keeping the terms in the action up to the second order with respect to the tunneling, we obtain an effective action for the phase difference across the junction:

$$\begin{aligned} S_J[\varphi^c, \varphi^q] &= \frac{i\hbar}{2} \int_{-\infty}^{+\infty} \sum_{kk'} \frac{\gamma_{kk'}}{\mathcal{V}_l \mathcal{V}_r} \text{Tr} \left[\mathbf{G}_{l,k}(t-t') \Gamma(\phi^c(t'), \phi^q(t')) \right. \\ &\quad \left. \times \mathbf{G}_{r,k'}(t'-t) \Gamma^\dagger(\phi^c(t), \phi^q(t)) \right] dt dt'. \end{aligned} \quad (41)$$

Assuming $\gamma_{kk'} = \gamma = \text{const}$, and a constant electronic density of states of the leads in their normal states, we evaluate summations over k and k' indices

$$\frac{\gamma}{\mathcal{V}_\alpha} \sum_k \mathbf{G}_{\alpha,k}(t-t') = \frac{1}{2} \pi \gamma N_\alpha \mathbf{g}_\alpha(t-t'), \quad (42)$$

where N_α is the density of states per the unit volume in the lead α at the Fermi level in its normal state. Quasiclassical Green's function of superconducting leads is given by [61]

$$\mathbf{g}_\alpha(t-t') = \frac{1}{\pi} \int_{-\infty}^{+\infty} \mathbf{G}_{\alpha,k}(t-t') d\xi_{\alpha,k}. \quad (43)$$

This Green's function has Keldysh causality structure

$$\mathbf{g}_\alpha(t-t') = \begin{bmatrix} \mathbf{g}_\alpha^K(t-t') & \mathbf{g}_\alpha^R(t-t') \\ \mathbf{g}_\alpha^A(t-t') & 0 \end{bmatrix}, \quad (44)$$

retarded, advanced, and Keldysh 2×2 blocks read as

$$\mathbf{g}_\alpha^{\text{R/A/K}}(t-t') = \begin{bmatrix} g_\alpha^{\text{R/A/K}}(t-t') & f_\alpha^{\text{R/A/K}}(t-t') \\ f_\alpha^{\text{R/A/K}}(t-t') & g_\alpha^{\text{R/A/K}}(t-t') \end{bmatrix}, \quad (45)$$

where Fourier images of retarded, advanced, and Keldysh components of normal and anomalous quasiclassical Green's functions are shown in (6). Then, Eq. (41) reduces to (2) accompanied with (5), where we have used an identity

$$\int_{-\infty}^{+\infty} f(t)g(-t)e^{i\omega t} dt = \int_{-\infty}^{+\infty} f(\omega')g(\omega'-\omega) \frac{d\omega}{2\pi}. \quad (46)$$

B Stochastic unraveling

We split action (2) into two terms which describe dissipation and fluctuations, respectively:

$$\begin{aligned} S_J[\varphi^c, \varphi^q] &= S_d[\varphi^c, \varphi^q] + S_f[\varphi^c, \varphi^q], \\ S_d[\varphi^c, \varphi^q] &= -\left(\frac{\Phi_0}{2\pi}\right)^2 \int_{-\infty}^{+\infty} \chi^{\text{q}\dagger}(t) \Pi^{\text{R}}(t-t') \chi^c(t') dt dt', \\ S_f[\varphi^c, \varphi^q] &= -\frac{1}{2} \left(\frac{\Phi_0}{2\pi}\right)^2 \int_{-\infty}^{+\infty} \chi^{\text{q}\dagger}(t) \Pi^{\text{K}}(t-t') \chi^q(t') dt dt'. \end{aligned} \quad (47)$$

Here, we used relation between retarded and advanced components of the polarization operators $\Pi^{\text{R}}(t-t') = \Pi^{\text{A}\dagger}(t'-t)$. We use Hubbard–Stratonovich transformation to the exponential of fluctuation action:

$$\begin{aligned} \exp\left(\frac{i}{\hbar} S_f[\varphi^c, \varphi^q]\right) &= \int \mathcal{D}[\xi, \xi^*] \exp\left[-\frac{1}{2} \int_{-\infty}^{+\infty} \xi^\dagger(t) \mathbf{D}(t-t') \xi(t) dt dt'\right] \\ &\quad \times \exp\left\{\frac{\Phi_0}{2\pi} \int_{-\infty}^{+\infty} [\xi^\dagger(t) \chi^q(t) + c.c.] dt\right\}, \end{aligned} \quad (48)$$

where the kernel $\mathbf{D}(t-t')$ in Fourier domain reads as

$$\mathbf{D}(\omega) = \left[\frac{i}{\hbar} \Pi^{\text{K}}(\omega)\right]^{-1}. \quad (49)$$

Since this kernel is positive-definite, the first exponential in (48) can be associated with a measure of stochastic Gaussian process $\xi(t)$ with two-point correlators (8). Collecting the factors, we obtain (9).

C Transmission coefficient

To calculate the transmission coefficient, we send a signal $v_p(t)$ to the probe line which is weakly coupled to the resonator. The equations of motion for the flux degrees of freedom in

the Fourier space read as:

$$\begin{aligned} \left[G_{r,0}^R(\omega; \varphi_0, V_0, \Omega) \right]^{-1} \phi_r(\omega) + \omega^2 C_p [\phi_r(\omega) - \phi_p(\omega)] &= 0, \\ \omega^2 C_p [\phi_p(\omega) - \phi_r(\omega)] + \frac{2i\omega}{Z_p} \phi_p(\omega) + \frac{2v_p(\omega)}{Z_p} &= 0. \end{aligned} \quad (50)$$

Since we are interested in the average field, we ignore the noise contribution here. Transmission coefficient $S_{21}(\omega)$ provides relation between the input field $v_p(\omega)$ and output field

$$v_o(\omega) = -i\omega\phi_p(\omega) = S_{21}(\omega)v_p(\omega). \quad (51)$$

This coefficient can be easily obtained by solving system (50). In the second order with respect to the coupling capacitance C_p , it is given by Eq. (29)

D Heat flow

To calculate the heat flow to the probe line, we take account of the noise current coming from the driven junction together with the thermal noise from the drive line. We start with equation of motion in time domain:

$$\begin{aligned} C_r \ddot{\phi}_r(t) + \int_{-\infty}^t Y_{J,0}(t-t'; \varphi_0, V_0, \Omega) \dot{\phi}_r(t') dt' + \frac{\phi_r(t)}{L_r} \\ + C_p [\ddot{\phi}_r(t) - \ddot{\phi}_p(t)] = -\tilde{I}_J(t; \varphi_0, V_0, \Omega), \\ C_p [\ddot{\phi}_p(t) - \ddot{\phi}_r(t)] + \frac{2\dot{\phi}_p(t)}{Z_p} = -\tilde{I}_p(t). \end{aligned} \quad (52)$$

Here, $\tilde{I}_p(t)$ is the thermal current noise from the transmission line, characterized by the correlation function

$$\int_{-\infty}^{+\infty} \langle \tilde{I}_p(t) \tilde{I}_p(0) \rangle e^{i\omega t} dt = \frac{2\hbar\omega}{Z_p} \coth\left(\frac{\hbar\omega}{2k_B T_p}\right). \quad (53)$$

To get expression for the heat flow power, we multiply the first equation by $\dot{\phi}_r$, the second equation by $\dot{\phi}_p$, add them up, and collect the terms which can be expressed as a full time derivative:

$$\frac{d}{dt} \left\{ \frac{C_r \dot{\phi}_r^2(t)}{2} + \frac{\phi_r^2(t)}{2L_r} + \frac{C_p [\dot{\phi}_r(t) - \dot{\phi}_p(t)]^2}{2} \right\} = W_J(t) + W_p(t), \quad (54)$$

where

$$\begin{aligned} W_J(t) &= -\dot{\phi}_r(t) \left[\tilde{I}_J(t; \varphi_0, V_0, \Omega) + \int_{-\infty}^t Y_{J,0}(t-t'; \varphi_0, V_0, \Omega) \dot{\phi}_r(t') dt' \right], \\ W_p(t) &= -\dot{\phi}_p(t) \left[\tilde{I}_p(t) + \frac{2\dot{\phi}_p(t)}{Z_p} \right]. \end{aligned} \quad (55)$$

Eq. (54) reflects energy conservation law, where the left hand side is a time derivative of the circuit energy, and the right hand side $W_J(t) + W_p(t)$ corresponds to the power coming to

the resonator from the junction and the probe, respectively. Then, we proceed with solving the Eqs. (52) for ϕ_p in the frequency domain. In the second order with respect to C_p , we obtain

$$-i\omega\phi_p(\omega) = \tilde{I}_p(\omega)Z_p \left[-\frac{1}{2} - \frac{iC_p Z_p \omega}{4} + \frac{C_p^2 Z_p^2 \omega^2}{8} + \frac{iC_p^2 G_{r,0}^R(\omega) Z_p \omega^3}{4} \right] \\ + \tilde{I}_J(\omega)Z_p C_p G_{r,0}^R(\omega) \omega^2 \left[-\frac{1}{2} - \frac{iC_p Z_p \omega}{4} + \frac{C_p G_{r,0}^R(\omega) \omega^2}{2} \right], \quad (56)$$

where we have omitted parameters of the drive in the resonator's Green's function for brevity. Taking into account that correlator of the junction noise current and probe noise vanishes, we average expression for the W_p over the noise realizations:

$$\langle W_p(\omega) \rangle = \frac{C_p^2 Z_p}{2} \int_{-\infty}^{+\infty} \left\{ \langle \tilde{I}_p(\omega') \tilde{I}_p(\omega - \omega') \rangle \frac{Z_p}{4} \left[i\omega'^3 G_{r,0}^R(\omega') + i(\omega - \omega')^3 G_{r,0}^R(\omega - \omega') \right] \right. \\ \left. + \frac{\omega^2 Z_p}{2} - \frac{i\omega}{C_p} \right\} - \langle \tilde{I}_J(\omega') \tilde{I}_J(\omega - \omega') \rangle \omega'^2 (\omega - \omega')^2 G_{r,0}^R(\omega') G_{r,0}^R(\omega - \omega') \frac{d\omega'}{2\pi}. \quad (57)$$

For the current noise correlation functions we have

$$\langle \tilde{I}_p(\omega') \tilde{I}_p(\omega - \omega') \rangle = 2\pi\delta(\omega) \frac{2\hbar\omega'}{Z_p} \coth\left(\frac{\hbar\omega'}{2k_B T_p}\right), \quad (58) \\ G_{r,0}(\omega') G_{r,0}(\omega - \omega') \langle \tilde{I}_J(\omega') \tilde{I}_J(\omega - \omega') \rangle = i\hbar \sum_{n=-\infty}^{+\infty} 2\pi\delta(\omega - n\Omega) G_{r,n}^K(\omega - \omega').$$

The Fourier image of the heat flow power presents a sum of evenly spaced delta-peaks, therefore it is a periodic function of time. Therefore, averaging over the time is equivalent to integration over vicinity of zero frequency:

$$\langle \overline{W_p} \rangle = \lim_{\varepsilon \rightarrow +0} \int_{-\varepsilon}^{\varepsilon} \langle W_p(\omega) \rangle \frac{d\omega}{2\pi}. \quad (59)$$

By substituting (58) into (57) and (59), we obtain expression (30) for the time and noise averaged heat power.

References

- [1] A. Wallraff, D. I. Schuster, A. Blais, L. Frunzio, R.-S. Huang, J. Majer, S. Kumar, S. M. Girvin and R. J. Schoelkopf, *Strong coupling of a single photon to a superconducting qubit using circuit quantum electrodynamics*, Nature **431**(7005), 162 (2004), doi:[10.1038/nature02851](https://doi.org/10.1038/nature02851).
- [2] A. Blais, S. M. Girvin and W. D. Oliver, *Quantum information processing and quantum optics with circuit quantum electrodynamics*, Nature Physics **16**(3), 247 (2020), doi:[10.1038/s41567-020-0806-z](https://doi.org/10.1038/s41567-020-0806-z).
- [3] A. Blais, A. L. Grimsmo, S. Girvin and A. Wallraff, *Circuit quantum electrodynamics*, Reviews of Modern Physics **93**(2), 025005 (2021), doi:[10.1103/revmodphys.93.025005](https://doi.org/10.1103/revmodphys.93.025005).

- [4] A. Blais, R.-S. Huang, A. Wallraff, S. M. Girvin and R. J. Schoelkopf, *Cavity quantum electrodynamics for superconducting electrical circuits: An architecture for quantum computation*, Physical Review A **69**(6), 062320 (2004), doi:[10.1103/physreva.69.062320](https://doi.org/10.1103/physreva.69.062320).
- [5] A. A. Clerk, K. W. Lehnert, P. Bertet, J. R. Petta and Y. Nakamura, *Hybrid quantum systems with circuit quantum electrodynamics*, Nature Physics **16**(3), 257 (2020), doi:[10.1038/s41567-020-0797-9](https://doi.org/10.1038/s41567-020-0797-9).
- [6] I. Carusotto, A. A. Houck, A. J. Kollár, P. Roushan, D. I. Schuster and J. Simon, *Photonic materials in circuit quantum electrodynamics*, Nature Physics **16**(3), 268 (2020), doi:[10.1038/s41567-020-0815-y](https://doi.org/10.1038/s41567-020-0815-y).
- [7] Y. Makhlin, G. Schön and A. Shnirman, *Quantum-state engineering with josephson-junction devices*, Reviews of Modern Physics **73**(2), 357 (2001), doi:[10.1103/revmodphys.73.357](https://doi.org/10.1103/revmodphys.73.357).
- [8] A. Schmid, *Diffusion and localization in a dissipative quantum system*, Physical Review Letters **51**(17), 1506 (1983), doi:[10.1103/physrevlett.51.1506](https://doi.org/10.1103/physrevlett.51.1506).
- [9] S. Bulgadaev, *Phase diagram of a dissipative quantum system*, JETP Lett **39**(6), 264 (1984).
- [10] J. S. Penttilä, Ü. Parts, P. J. Hakonen, M. A. Paalanen and E. B. Sonin, “*superconductor-insulator transition*” in a single josephson junction, Physical Review Letters **82**(5), 1004 (1999), doi:[10.1103/physrevlett.82.1004](https://doi.org/10.1103/physrevlett.82.1004).
- [11] A. Murani, N. Bourlet, H. le Sueur, F. Portier, C. Altimiras, D. Esteve, H. Grabert, J. Stockburger, J. Ankerhold and P. Joyez, *Absence of a dissipative quantum phase transition in josephson junctions*, Physical Review X **10**(2), 021003 (2020), doi:[10.1103/physrevx.10.021003](https://doi.org/10.1103/physrevx.10.021003).
- [12] R. Kuzmin, N. Mehta, N. Grabon, R. A. Mencia, A. Burshtein, M. Goldstein and V. E. Manucharyan, *Observation of the schmid–bulgadaev dissipative quantum phase transition*, Nature Physics **21**(1), 132 (2024), doi:[10.1038/s41567-024-02695-7](https://doi.org/10.1038/s41567-024-02695-7).
- [13] F. Giazotto, T. T. Heikkilä, A. Luukanen, A. M. Savin and J. P. Pekola, *Opportunities for mesoscopics in thermometry and refrigeration: Physics and applications*, Reviews of Modern Physics **78**(1), 217 (2006), doi:[10.1103/revmodphys.78.217](https://doi.org/10.1103/revmodphys.78.217).
- [14] J. P. Pekola, *Towards quantum thermodynamics in electronic circuits*, Nature Physics **11**(2), 118 (2015), doi:[10.1038/nphys3169](https://doi.org/10.1038/nphys3169).
- [15] M. Partanen, K. Y. Tan, J. Govenius, R. E. Lake, M. K. Mäkelä, T. Tanttu and M. Möttönen, *Quantum-limited heat conduction over macroscopic distances*, Nature Physics **12**(5), 460 (2016), doi:[10.1038/nphys3642](https://doi.org/10.1038/nphys3642).
- [16] J. P. Pekola and B. Karimi, *Colloquium: Quantum heat transport in condensed matter systems*, Reviews of Modern Physics **93**(4), 041001 (2021), doi:[10.1103/revmodphys.93.041001](https://doi.org/10.1103/revmodphys.93.041001).
- [17] L. Arrachea, *Energy dynamics, heat production and heat–work conversion with qubits: toward the development of quantum machines*, Reports on Progress in Physics **86**(3), 036501 (2023), doi:[10.1088/1361-6633/acb06b](https://doi.org/10.1088/1361-6633/acb06b).
- [18] S. Schmidt and J. Koch, *Circuit qed lattices: Towards quantum simulation with superconducting circuits*, Annalen der Physik **525**(6), 395 (2013), doi:[10.1002/andp.201200261](https://doi.org/10.1002/andp.201200261).

- [19] B. M. Anderson, R. Ma, C. Owens, D. I. Schuster and J. Simon, *Engineering topological many-body materials in microwave cavity arrays*, Physical Review X **6**(4), 041043 (2016), doi:[10.1103/physrevx.6.041043](https://doi.org/10.1103/physrevx.6.041043).
- [20] A. J. Kollár, M. Fitzpatrick and A. A. Houck, *Hyperbolic lattices in circuit quantum electrodynamics*, Nature **571**(7763), 45 (2019), doi:[10.1038/s41586-019-1348-3](https://doi.org/10.1038/s41586-019-1348-3).
- [21] A. L. Grimsmo, B. Royer, J. M. Kreikebaum, Y. Ye, K. O'Brien, I. Siddiqi and A. Blais, *Quantum metamaterial for broadband detection of single microwave photons*, Physical Review Applied **15**(3), 034074 (2021), doi:[10.1103/physrevapplied.15.034074](https://doi.org/10.1103/physrevapplied.15.034074).
- [22] M. A. Dobbs, M. Lueker, K. A. Aird, A. N. Bender, B. A. Benson, L. E. Bleem, J. E. Carlstrom, C. L. Chang, H.-M. Cho, J. Clarke, T. M. Crawford, A. T. Crites *et al.*, *Frequency multiplexed superconducting quantum interference device readout of large bolometer arrays for cosmic microwave background measurements*, Review of Scientific Instruments **83**(7) (2012), doi:[10.1063/1.4737629](https://doi.org/10.1063/1.4737629).
- [23] J. Govenius, R. E. Lake, K. Y. Tan, V. Pietilä, J. K. Julin, I. J. Maasilta, P. Virtanen and M. Möttönen, *Microwave nanobolometer based on proximity josephson junctions*, Physical Review B **90**(6), 064505 (2014), doi:[10.1103/physrevb.90.064505](https://doi.org/10.1103/physrevb.90.064505).
- [24] R. Kokkonen, J.-P. Girard, D. Hazra, A. Laitinen, J. Govenius, R. E. Lake, I. Sallinen, V. Vesterinen, M. Partanen, J. Y. Tan, K. W. Chan, K. Y. Tan *et al.*, *Bolometer operating at the threshold for circuit quantum electrodynamics*, Nature **586**(7827), 47 (2020), doi:[10.1038/s41586-020-2753-3](https://doi.org/10.1038/s41586-020-2753-3).
- [25] A. M. Gunyhó, S. Kundu, J. Ma, W. Liu, S. Niemelä, G. Catto, V. Vadimov, V. Vesterinen, P. Singh, Q. Chen and M. Möttönen, *Single-shot readout of a superconducting qubit using a thermal detector*, Nature Electronics **7**(4), 288 (2024), doi:[10.1038/s41928-024-01147-7](https://doi.org/10.1038/s41928-024-01147-7).
- [26] C. Degen, F. Reinhard and P. Cappellaro, *Quantum sensing*, Reviews of Modern Physics **89**(3), 035002 (2017), doi:[10.1103/revmodphys.89.035002](https://doi.org/10.1103/revmodphys.89.035002).
- [27] A. Schneider, *Quantum sensing experiments with superconducting qubits*, KIT Scientific Publishing (2021).
- [28] S. Danilin, N. Nugent and M. Weides, *Quantum sensing with tunable superconducting qubits: optimization and speed-up*, New Journal of Physics **26**(10), 103029 (2024), doi:[10.1088/1367-2630/ad49c5](https://doi.org/10.1088/1367-2630/ad49c5).
- [29] M. H. Devoret and R. J. Schoelkopf, *Superconducting circuits for quantum information: An outlook*, Science **339**(6124), 1169 (2013), doi:[10.1126/science.1231930](https://doi.org/10.1126/science.1231930).
- [30] G. Wendin, *Quantum information processing with superconducting circuits: a review*, Reports on Progress in Physics **80**(10), 106001 (2017), doi:[10.1088/1361-6633/aa7e1a](https://doi.org/10.1088/1361-6633/aa7e1a).
- [31] P. Krantz, M. Kjaergaard, F. Yan, T. P. Orlando, S. Gustavsson and W. D. Oliver, *A quantum engineer's guide to superconducting qubits*, Applied Physics Reviews **6**(2) (2019), doi:[10.1063/1.5089550](https://doi.org/10.1063/1.5089550).
- [32] B. Josephson, *Possible new effects in superconductive tunnelling*, Physics Letters **1**(7), 251 (1962), doi:[10.1016/0031-9163\(62\)91369-0](https://doi.org/10.1016/0031-9163(62)91369-0).
- [33] B. D. Josephson, *The discovery of tunnelling supercurrents*, Reviews of Modern Physics **46**(2), 251 (1974), doi:[10.1103/revmodphys.46.251](https://doi.org/10.1103/revmodphys.46.251).

- [34] M. Tinkham, *Introduction to superconductivity*, vol. 1, Courier Corporation (2004).
- [35] A. I. Larkin and Y. N. Ovchinnikov, *Tunnel effect between superconductors in an alternating field*, Sov. Phys. JETP **24**(11), 1035 (1967).
- [36] Y. M. Ivanchenko, *Tunneling between two superconductors*, Sov. Phys. JETP **24**(1), 225 (1967).
- [37] M. Houzet, K. Serniak, G. Catelani, M. Devoret and L. Glazman, *Photon-assisted charge-parity jumps in a superconducting qubit*, Physical Review Letters **123**(10), 107704 (2019), doi:[10.1103/physrevlett.123.107704](https://doi.org/10.1103/physrevlett.123.107704).
- [38] A. Anferov, F. Wan, S. P. Harvey, J. Simon and D. I. Schuster, *A millimeter-wave superconducting qubit*, doi:[10.48550/ARXIV.2411.11170](https://doi.org/10.48550/ARXIV.2411.11170) (2024).
- [39] A. Anferov, S. P. Harvey, F. Wan, J. Simon and D. I. Schuster, *Superconducting qubits above 20 ghz operating over 200 mk*, PRX Quantum **5**(3), 030347 (2024), doi:[10.1103/prxquantum.5.030347](https://doi.org/10.1103/prxquantum.5.030347).
- [40] R. Lescanne, L. Verney, Q. Ficheux, M. H. Devoret, B. Huard, M. Mirrahimi and Z. Leghtas, *Escape of a driven quantum josephson circuit into unconfined states*, Physical Review Applied **11**(1), 014030 (2019), doi:[10.1103/physrevapplied.11.014030](https://doi.org/10.1103/physrevapplied.11.014030).
- [41] L. Verney, R. Lescanne, M. H. Devoret, Z. Leghtas and M. Mirrahimi, *Structural instability of driven josephson circuits prevented by an inductive shunt*, Physical Review Applied **11**(2), 024003 (2019), doi:[10.1103/physrevapplied.11.024003](https://doi.org/10.1103/physrevapplied.11.024003).
- [42] D. P. DiVincenzo, *The physical implementation of quantum computation*, Fortschritte der Physik **48**(9-11), 771 (2000), doi:[10.1002/1521-3978\(200009\)48:9/11<771::aid-prop771>3.0.co;2-e](https://doi.org/10.1002/1521-3978(200009)48:9/11<771::aid-prop771>3.0.co;2-e).
- [43] V. A. Sevriuk, W. Liu, J. Rönkkö, H. Hsu, F. Marxer, T. F. Mörstedt, M. Partanen, J. Rabinä, M. Venkatesh, J. Hotari, L. Grönberg, J. Heinsoo *et al.*, *Initial experimental results on a superconducting-qubit reset based on photon-assisted quasiparticle tunneling*, Applied Physics Letters **121**(23) (2022), doi:[10.1063/5.0129345](https://doi.org/10.1063/5.0129345).
- [44] T. Yoshioka, H. Mukai, A. Tomonaga, S. Takada, Y. Okazaki, N.-H. Kaneko, S. Nakamura and J.-S. Tsai, *Active initialization experiment of a superconducting qubit using a quantum circuit refrigerator*, Physical Review Applied **20**(4), 044077 (2023), doi:[10.1103/physrevapplied.20.044077](https://doi.org/10.1103/physrevapplied.20.044077).
- [45] A. Viitanen, T. Mörstedt, W. S. Teixeira, M. Tiiri, J. Rabinä, M. Silveri and M. Möttönen, *Quantum-circuit refrigeration of a superconducting microwave resonator well below a single quantum* (2023), [quant-ph2308.00397](https://arxiv.org/abs/2308.00397).
- [46] W. Teixeira, T. Mörstedt, A. Viitanen, H. Kivijärvi, A. Gunyhó, M. Tiiri, S. Kundu, A. Sah, V. Vadimov and M. Möttönen, *Many-excitation removal of a transmon qubit using a single-junction quantum-circuit refrigerator and a two-tone microwave drive*, Scientific Reports **14**(1) (2024), doi:[10.1038/s41598-024-64496-5](https://doi.org/10.1038/s41598-024-64496-5).
- [47] S. Nakamura, T. Yoshioka, S. Lemziakov, D. Lvov, H. Mukai, A. Tomonaga, S. Takada, Y. Okazaki, N.-H. Kaneko, J. Pekola and J.-S. Tsai, *Probing fast quantum circuit refrigeration in the quantum regime*, Physical Review Applied **23**(1), 1011003 (2025), doi:[10.1103/physrevapplied.23.1011003](https://doi.org/10.1103/physrevapplied.23.1011003).

- [48] K. Y. Tan, M. Partanen, R. E. Lake, J. Govenius, S. Masuda and M. Möttönen, *Quantum circuit refrigerator*, Nature Communications 8, 15189 (2017) (2016), doi:[10.1038/ncomms15189](https://doi.org/10.1038/ncomms15189), [1606.04728](https://arxiv.org/abs/1606.04728).
- [49] M. Silveri, H. Grabert, S. Masuda, K. Y. Tan and M. Möttönen, *Theory of quantum-circuit refrigeration by photon-assisted electron tunneling*, Phys. Rev. B **96**, 094524 (2017), doi:[10.1103/PhysRevB.96.094524](https://doi.org/10.1103/PhysRevB.96.094524), [1706.07188](https://arxiv.org/abs/1706.07188).
- [50] T. F. Mörstedt, A. Viitanen, V. Vadimov, V. Sevriuk, M. Partanen, E. Hyyppä, G. Catelani, M. Silveri, K. Y. Tan and M. Möttönen, *Recent developments in quantum-circuit refrigeration*, Annalen der Physik 534, 2100543 (2022) (2021), doi:[10.1002/andp.202100543](https://doi.org/10.1002/andp.202100543), [2111.11234](https://arxiv.org/abs/2111.11234).
- [51] V. Vadimov, A. Viitanen, T. Mörstedt, T. Ala-Nissila and M. Möttönen, *Single-junction quantum-circuit refrigerator*, AIP Advances **12**, 075005 (2022), doi:[https://doi.org/10.1063/5.0096849](https://doi.org/https://doi.org/10.1063/5.0096849), [2112.08008](https://arxiv.org/abs/2112.08008).
- [52] T. F. Mörstedt, W. S. Teixeira, A. Viitanen, H. Kivijärvi, M. Tiiri, M. Rasola, A. M. Gunyho, S. Kundu, L. Lattier, V. Vadimov, G. Catelani, V. Sevriuk *et al.*, *Rapid on-demand generation of thermal states in superconducting quantum circuits*, doi:[10.48550/ARXIV.2402.09594](https://doi.org/10.48550/ARXIV.2402.09594) (2024).
- [53] T. Uusnäkki, T. Mörstedt, W. Teixeira, M. Rasola and M. Möttönen, *Experimental realization of a quantum heat engine based on dissipation-engineered superconducting circuits*, doi:[10.48550/ARXIV.2502.20143](https://doi.org/10.48550/ARXIV.2502.20143) (2025).
- [54] H. Hsu, M. Silveri, A. Gunyhó, J. Goetz, G. Catelani and M. Möttönen, *Tunable refrigerator for non-linear quantum electric circuits*, Phys. Rev. B **101**, 235422 (2020), doi:[10.1103/PhysRevB.101.235422](https://doi.org/10.1103/PhysRevB.101.235422), [2002.06867](https://arxiv.org/abs/2002.06867).
- [55] A. Viitanen, M. Silveri, M. Jenei, V. Sevriuk, K. Y. Tan, M. Partanen, J. Goetz, L. Grönberg, V. Vadimov, V. Lahtinen and M. Möttönen, *Photon-number-dependent effective lamb shift*, Physical Review Research **3**(3), 033126 (2021), doi:[10.1103/physrevresearch.3.033126](https://doi.org/10.1103/physrevresearch.3.033126).
- [56] H. Kivijärvi, A. Viitanen, T. Mörstedt and M. Möttönen, *Noise-induced quantum-circuit refrigeration*, doi:[10.48550/ARXIV.2412.05886](https://doi.org/10.48550/ARXIV.2412.05886) (2024).
- [57] J. P. Pekola and F. W. J. Hekking, *Normal-metal-superconductor tunnel junction as a brownian refrigerator*, Physical Review Letters **98**(21), 210604 (2007), doi:[10.1103/physrevlett.98.210604](https://doi.org/10.1103/physrevlett.98.210604).
- [58] J. Estève, M. Aprili and J. Gabelli, *Quantum dynamics of a microwave resonator strongly coupled to a tunnel junction*, doi:[10.48550/ARXIV.1807.02364](https://doi.org/10.48550/ARXIV.1807.02364) (2018).
- [59] G. Aiello, M. Féchant, A. Morvan, J. Basset, M. Aprili, J. Gabelli and J. Estève, *Quantum bath engineering of a high impedance microwave mode through quasiparticle tunneling*, Nature Communications **13**(1) (2022), doi:[10.1038/s41467-022-34762-z](https://doi.org/10.1038/s41467-022-34762-z).
- [60] O. Stanisavljević, J.-C. Philippe, J. Gabelli, M. Aprili, J. Estève and J. Basset, *Efficient microwave photon-to-electron conversion in a high-impedance quantum circuit*, Physical Review Letters **133**(7), 076302 (2024), doi:[10.1103/physrevlett.133.076302](https://doi.org/10.1103/physrevlett.133.076302).
- [61] N. B. Kopnin, *Theory of nonequilibrium superconductivity*, vol. 110, Oxford University Press (2001).

- [62] G.-L. Ingold and Y. V. Nazarov, *Charge Tunneling Rates in Ultrasmall Junctions*, pp. 21–107, Springer US, ISBN 9781475721669, doi:[10.1007/978-1-4757-2166-9_2](https://doi.org/10.1007/978-1-4757-2166-9_2) (1992).
- [63] A. Ciani, D. P. DiVincenzo and B. M. Terhal, *Lecture Notes on Quantum Electrical Circuits*, TU Delft OPEN Publishing, ISBN 9789463668149, doi:[10.59490/tb.85](https://doi.org/10.59490/tb.85) (2024).
- [64] V. Ambegaokar, U. Eckern and G. Schön, *Quantum dynamics of tunneling between superconductors*, *Physical Review Letters* **48**(25), 1745 (1982), doi:[10.1103/physrevlett.48.1745](https://doi.org/10.1103/physrevlett.48.1745).
- [65] U. Eckern, G. Schön and V. Ambegaokar, *Quantum dynamics of a superconducting tunnel junction*, *Physical Review B* **30**(11), 6419 (1984), doi:[10.1103/physrevb.30.6419](https://doi.org/10.1103/physrevb.30.6419).
- [66] G. Schön and A. Zaikin, *Quantum coherent effects, phase transitions, and the dissipative dynamics of ultra small tunnel junctions*, *Physics Reports* **198**(5-6), 237 (1990), doi:[10.1016/0370-1573\(90\)90156-v](https://doi.org/10.1016/0370-1573(90)90156-v).
- [67] A. Kamenev, *Field theory of non-equilibrium systems*, Cambridge University Press (2023).
- [68] J. S. Toll, *Causality and the dispersion relation: Logical foundations*, *Physical Review* **104**(6), 1760 (1956), doi:[10.1103/physrev.104.1760](https://doi.org/10.1103/physrev.104.1760).
- [69] G. Catelani, J. Koch, L. Frunzio, R. J. Schoelkopf, M. H. Devoret and L. I. Glazman, *Quasiparticle relaxation of superconducting qubits in the presence of flux*, *Physical Review Letters* **106**(7), 077002 (2011), doi:[10.1103/physrevlett.106.077002](https://doi.org/10.1103/physrevlett.106.077002).
- [70] G. Catelani, *Parity switching and decoherence by quasiparticles in single-junction transmons*, *Physical Review B* **89**(9), 094522 (2014), doi:[10.1103/physrevb.89.094522](https://doi.org/10.1103/physrevb.89.094522).
- [71] G. Marchegiani, L. Amico and G. Catelani, *Quasiparticles in superconducting qubits with asymmetric junctions*, *PRX Quantum* **3**(4), 040338 (2022), doi:[10.1103/prxquantum.3.040338](https://doi.org/10.1103/prxquantum.3.040338).
- [72] S. Diamond, V. Fatemi, M. Hays, H. Nho, P. D. Kurilovich, T. Connolly, V. R. Joshi, K. Serniak, L. Frunzio, L. I. Glazman and M. H. Devoret, *Distinguishing parity-switching mechanisms in a superconducting qubit*, *PRX Quantum* **3**(4), 040304 (2022), doi:[10.1103/prxquantum.3.040304](https://doi.org/10.1103/prxquantum.3.040304).
- [73] J. Hubbard, *Calculation of partition functions*, *Physical Review Letters* **3**(2), 77 (1959), doi:[10.1103/physrevlett.3.77](https://doi.org/10.1103/physrevlett.3.77).
- [74] R. Stratonovich, *On a method of calculating quantum distribution functions*, *Soviet Physics Doklady* **2**, 416 (1957).
- [75] A. Schmid, *On a quasiclassical langevin equation*, *Journal of Low Temperature Physics* **49**(5-6), 609 (1982), doi:[10.1007/bf00681904](https://doi.org/10.1007/bf00681904).
- [76] V. Ambegaokar and A. Baratoff, *Tunneling between superconductors*, *Physical Review Letters* **10**(11), 486 (1963), doi:[10.1103/physrevlett.10.486](https://doi.org/10.1103/physrevlett.10.486).
- [77] L. Glazman and G. Catelani, *Bogoliubov quasiparticles in superconducting qubits*, *SciPost Physics Lecture Notes* (2021), doi:[10.21468/scipostphyslectnotes.31](https://doi.org/10.21468/scipostphyslectnotes.31).
- [78] I. M. Pop, K. Geerlings, G. Catelani, R. J. Schoelkopf, L. I. Glazman and M. H. Devoret, *Coherent suppression of electromagnetic dissipation due to superconducting quasiparticles*, *Nature* **508**(7496), 369 (2014), doi:[10.1038/nature13017](https://doi.org/10.1038/nature13017).

- [79] M. Xu, Y. Yan, Q. Shi, J. Ankerhold and J. Stockburger, *Taming quantum noise for efficient low temperature simulations of open quantum systems*, Physical Review Letters **129**(23), 230601 (2022), doi:[10.1103/physrevlett.129.230601](https://doi.org/10.1103/physrevlett.129.230601).
- [80] M. Xu, V. Vadimov, M. Krug, J. T. Stockburger and J. Ankerhold, *A universal framework for quantum dissipation: minimally extended state space and exact time-local dynamics*, doi:[10.48550/ARXIV.2307.16790](https://doi.org/10.48550/ARXIV.2307.16790) (2023), [2307.16790](https://arxiv.org/abs/2307.16790).
- [81] V. Vadimov, M. Xu, J. T. Stockburger, J. Ankerhold and M. Möttönen, *Nonlinear-response theory for lossy superconducting quantum circuits*, Physical Review Research **7**(1), 013317 (2025), doi:[10.1103/physrevresearch.7.013317](https://doi.org/10.1103/physrevresearch.7.013317).